

PAPER • OPEN ACCESS

Pulsed Nd:YAG deposition of nanostructured FeS_{1-x} containing meta-stable phases

To cite this article: T Kenek *et al* 2017 *IOP Conf. Ser.: Mater. Sci. Eng.* **175** 012022

View the [article online](#) for updates and enhancements.

Related content

- [The large-scale synthesis and characterization of carbon nanotubes filled with longcontinuous inorganic nanowires in supercritical \$\text{CO}_2\$](#)
Wei Luo, Yi Xie, Kun Zhu et al.
- [Iron sulfide ink for the growth of pyrite crystals](#)
Alec Kirkeminde, Phillip Gingrich, Maogang Gong et al.
- [Halide vapor phase epitaxy of twin-free \$\text{Ga}_2\text{O}_3\$ on sapphire \(0001\) substrates](#)
Yuichi Oshima, Encarnación G. Villora and Kiyoshi Shimamura

Pulsed Nd:YAG deposition of nanostructured FeS_{1-x} containing meta-stable phases

T Křenek^{1*}, S Karatodorov², R Medlín¹, V Mihailov², J Savková¹

¹University of West Bohemia, Research Centre New Technologies 30614 Plzen, Czech Republic

²Institute of Solid State Physics - Bulgarian Academy of Sciences, 1784 Sofia, Bulgaria

E-mail: tkrenek@ntc.zcu.cz

Abstract. Pulsed near-IR laser irradiation of ferrous sulfide (FeS) in a vacuum allows a non-congruent ablation and deposition of nanostructured FeS_{1-x} thin films. Deposition has been performed on Al, Ta and Cu unheated substrate and analyzed by scanning (SEM) and high resolution transmission electron microscopy (HRTEM) and electron diffraction. Morphologically, the similar homogeneous, dark, metallic and adhesive appearances have been revealed for all the coats deposited on various substrates (by SEM). However, using HRTEM in agreement with electron diffraction, different phase composition on various substrates has been detected. Cubic pyrite phase (FeS_2) has been detected on Ta substrate. Cubic pyrite (FeS_2) and metastable rhomboedric smythite Fe_9S_{11} have been found in case of Al substrate. Cubic pyrite (FeS_2), metastable rhomboedric smythite Fe_9S_{11} and metastable orthorhombic marcasite (FeS_{2m}) revealed HRTEM analysis of the film on Cu substrate. In case of all deposits the detected crystalline nanograins were surrounded by amorphous matrix.

1. Introduction

Iron sulfide thin films attract attention because of its potential application for solar cell materials [eg. 1] and due to interesting electrical semiconducting [eg. 2] and magnetic [eg. 3] properties of this material. Although another solar cell materials (eg. such as cadmium, lead, indium or selenium) exhibit higher efficiencies, FeS non-toxicity, abundance, and cheap price make this candidate attractive. The iron sulfide (Fe-S) system represents a complex phase diagram including seven phases: pyrite (cubic- FeS_2), marcasite (calcium chloride structure- FeS_2), pyrrhotite-IT (Fe_{1-x}S), pyrrhotite-4M (Fe_7S_8), Fe_9S_{10} , greigite (cubic spinel- Fe_3S_4), troilite- 2H (FeS) and mackinawite (Fe_{1+x}S) [4]. Only pyrite (FeS_{2p}) and pyrrhotite (Fe_{1-x}) are stable.

Iron sulfide thin coats have been obtained by ion beam and reactive sputtering (FeS_2) [5], vacuum thermal evaporation (FeS_2) [6], chemical spray pyrolysis (FeS_2) [7], sulfurization of iron oxides to FeS_2 [8], atmospheric-or low-pressure metal-organic chemical vapor deposition (AP or LP MOCVD; FeS_2) [eg.9], FeS_2 thin films using LPCVD of iron pentacarbonyl [$\text{Fe}(\text{CO})_5$] hydrogensulfide, and *tert*-butyl sulfide as precursors [10] and flash evaporation (FeS_2) [11]. Iron sulfide nanoparticles were prepared using high-energy mechanical milling [12].

There have been published only few studies on laser ablative deposition of iron sulfide were interaction of reactive collisions with unheated substrate surfaces, were explored. The laser ablative



deposition of pyrite (FeS_2) on aluminium and silica substrates resulted in the deposition of films including FeS constituents under the both higher and room temperature [13].

Recently we have reported on the pulsed IR laser ablative deposition of ferrous sulfide FeS on unheated silica, tantalum and copper substrates [14]. Herein we continue on near-IR Nd:YAG pulsed laser deposition on unheated Al, Ta, Cu substrates.

2. Experimental

The 1064 nm near IR laser irradiation and deposition experiments are conducted in 10^{-2} Torr vacuum in a metal reactor with 343 mL volume. The metal reactor[15] has three borosilicate glass windows and it is connected to vacuum manifold and pressure transducer. The vacuum system used is Lavat AV 63. For the deposition, we use a pulsed Nd:YAG Quanta Ray GCR3 laser. The pulse duration at 1064 nm is 8 ns and the pulse energies used are up to 165 mJ. The repetition frequency is set to the maximum value of 20 Hz and the number of pulses for each sample is 2500. The radiation is focused with a 25 cm focal distance glass lens, producing up to 600 Jcm^{-2} energy fluence at the target surface. The target is a FeS pellet with diameter 8 mm and height 5 mm positioned in the centre of the reactor. The substrate is positioned vertically above the target on top of a 9.5 cm diameter glass cylinder. Three different types of substrates are used: tantalum, aluminium and copper foils. Each metal substrate is pierced in the middle to allow the passing of the laser beam.

Transmission electron microscopy (TEM) analysis (particle size and phase analysis) was carried out with a Transmission Electron Microscope JEM 2200FS (Shottky) from JEOL operated at 200 kV with CCD Gatan (Digital Micrograph software), in-column Omega energy filter for EFTEM and EELS analysis, STEM mode with HAADF detector and EDS 80 mm^2 SDD (Silicon Drift Detector) X-Max detector from Oxford Instruments. Samples that were subsequently dispersed in ethanol followed by the application of a drop of diluted suspension on a polymer/carbon coated Cu grid. The diffraction patterns were evaluated using the database JCPDS-2 and ProcessDiffraction software package [16]. Scanning Electron Microscope (SEM) analysis was carried out with a JEOL JSM 7600F autoemission microscope with EPMA 50 mm^2 SDD X-MAX EDS. The FeS pellet was made at 100 atm. on a hydraulic press from a commercially available iron sulfide powder (FeS, 99% Fe, Aldrich).

3. Results and discussion

The near IR laser irradiation of the FeS pellet in the vacuum leads to the pellet ablation and to the formation of visible luminescence (plasma) zone exhibits as a bluish plume which is filling whole glass cylinder [15]. The highly focused pulsed laser irradiation of FeS pellet caused creation of crater of ejected particles on adjacent of Ta, Al, Cu, where they are deposited as solid films. The coats on all selected substrates exhibit the same homogeneous, dark, metallic and adhesive appearances.

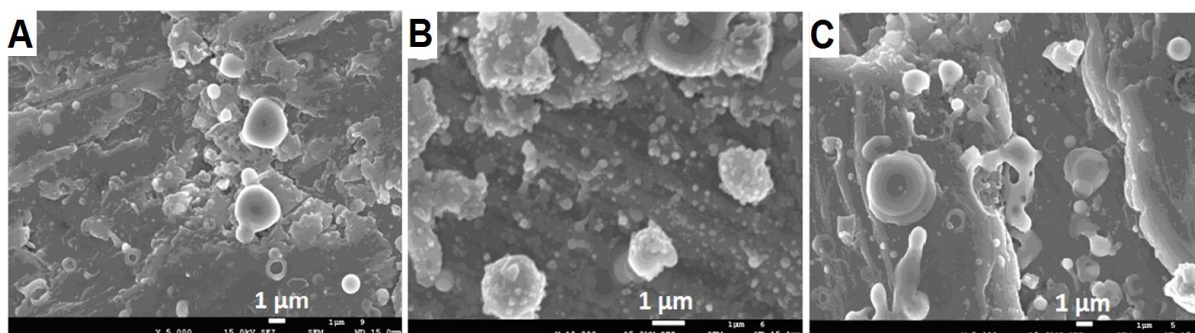


Figure 1. Morphology of FeS deposits on (A) aluminium, (B) copper, (C) tantalum substrate

The SEM images (Figure 1) of the coats deposited on Al (Figure 1 A), Cu (Figure 1 B) and Ta (Figure 1 C) show round-shaped particles which dimension span from tens of nm up to units of μm on the flat discontinuous areas. EDX analyses revealed similar composition of all three samples. Round shaped

particles, flat areas as well as ring-like objects exhibit heterogeneous composition with deficient of S. The S/Fe atomic percent ratio spans from 1:1 up to 1:2. The X-ray diffraction analysis of the commercial FeS sample allows the estimation of the relative amounts of crystalline troilite (~63%), pyrrhotite (~24%) and alpha-Fe (13%) it contains [14].

The phase composition of the prepared samples was studied by electron diffraction. The electron diffraction (Figure 2 A) of FeS deposit on Ta substrate which is generally considered as an inert substrate reveals the presence of stable cubic pyrite (JCPDS file 00-001-1295) phase. The HRTEM image (Figure 2 B) shows partially crystallized structure with interlayer spacing $d = 0.192$ nm which corresponds with cubic pyrite interplanar distance 220, according to JCPDS PDF 00-001-1295. From the HRTEM image is visible that the deposit has amorphous matrix with many small nanocrystals with the size about 3-5 nm.

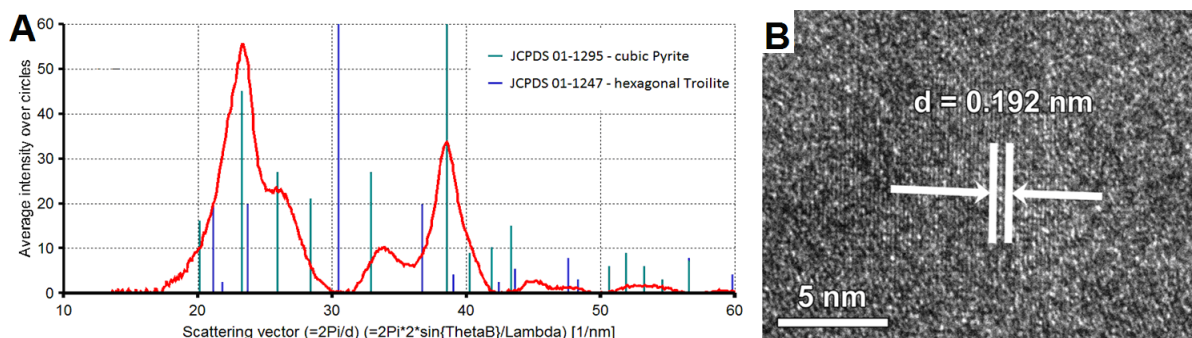


Figure 2. (A) Electron diffraction of FeS deposit on Ta substrate, (B) HRTEM image of FeS deposit on Ta substrate depicting cubic pyrite FeS_2 phase

The FeS thin film deposit on aluminium substrate exhibits the presence of two crystalline phases. In agreement with electron diffraction (Figure 3 A) the deposit consists of stable FeS_2 cubic pyrite (01-1295) and interestingly of unstable Fe_9S_{11} rhombohedral smythite phase (JCPDS 10-0437). The phases show HRTEM images (figure 3B, C) where interlayer spacing $d = 0.295$ nm (012) and $d = 0.270$ nm (200) corresponds with smythite phase and pyrite phase respectively.

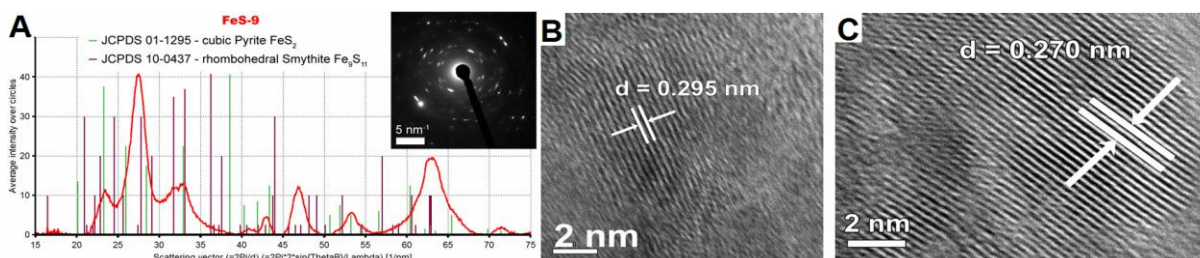


Figure 3. (A) Electron diffraction of FeS deposit on Al substrate; (B) HRTEM image of FeS deposit on Al substrate depicting unstable Fe_9S_{11} rhombohedral smythite and (C) cubic pyrite FeS_2 phase

Ablative deposition on copper substrate led to the formation of highly multiphase structure composed of FeS_2 cubic pyrite, unstable Fe_9S_{11} rhombohedral smythite and FeS_2 orthorhombic marcasite (JCPDS 00-003-0799). Electron diffraction assignment is given in Figure 4 A. The presence of unstable FeS phases confirm also HRTEM analyses (Figure 4 B, C) whose using allowed detection of $d = 0.258$ nm and $d = 0.169$ nm interlayer spacing which fits with rhombohedral smythite (107) and orthorhombic marcasite phase (002) respectively.

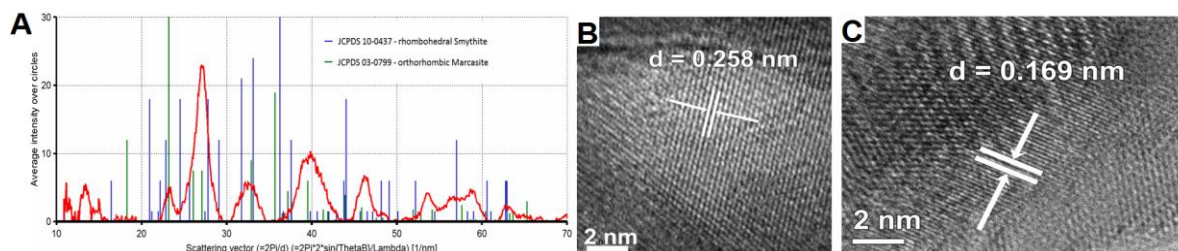


Figure 4.(A) Electron diffraction of FeS deposit on Cu substrate; HRTEM image of FeS deposit on Ta substrate depicting (B) unstable Fe_9S_{11} rhombohedral smythite, (C) FeS_2 orthorhombic marcasite phase (002)

4. Conclusion

Pulsed near-IR laser deposition of FeS in a vacuum on Al, Ta and Cu substrate has been performed and the thin films were analysed by scanning (SEM) and high resolution transmission electron (HRTEM) microscopy and electron diffraction. SEM analysis revealed homogeneous, dark, metallic deposit round-shaped and ring-like particles. Via HRTEM and electron diffraction have been detected stable cubic pyrite phase (FeS_2) on Ta, Cu and Al substrate, metastable rhomboedric smythite Fe_9S_{11} on Al and Cu substrate and metastable orthorhombic marcasite (FeS_{2m}) on Cu substrate. These results represent the first examples of ablative deposition of unstable crystalline phases of ferrous sulfide.

Acknowledgements

The result was developed within the CENTEM project, reg. no. CZ.1.05/2.1.00/03.0088, cofounded by the ERDF as part of the Ministry of Education, Youth and Sports OP RDI programme and, in the follow-up sustainability stage, supported through CENTEM PLUS (LO1402) by financial means from the Ministry of Education, Youth and Sports under the National Sustainability Programme I and the project INERA (REGPOT-2012-2013-1).

References

- [1] Hofmann W K, Birkholz M 1990 *Solar Energy Materials* **20** 149
- [2] Lehner S W, Savage K S, Ayers J C 2006 *Journal of Crystal Growth* **286** 306
- [3] Takahashi T 1973 *Solid State Communications* **13** (9) 1335
- [4] Soon J M, Goh L Y, Loh K P 2007 *Applied Physics Letters* **91** 084105-1.
- [5] Birkholz M, Lichtenberger D, Hoepfner C, Fiechter S 1992 *Solar Energy Materials and Solar Cells* **27** 243
- [6] Rezig B, Dalma H, Kanzai M 1992 *Renewable Energy* **2** 25
- [7] Smestad G, Da Silva A, Tributsch H, Fiechter S, Kunst M, Meziani N, Birkholz M 1989 *Solar Energy Materials* **18** 299
- [8] Smestad G, Ennaoui E, Fiechter S, Tributsch H, Hofman W K, Birkholz M 1990 *Solar Energy Materials* **20** 149
- [9] Thomas B, Cibik T, Hoepfner C, Diesner D, Ehlers G, Fiechter S, Ellmer K 1998 *Journal of Materials Science* **9** 61
- [10] Schleigh D M H, Chang S W 1991 *Journal of Crystal Growth* **112** 737
- [11] Ferrer IJ, Sanchez C 1991 *Journal of Applied Physics* **70** 2641
- [12] Chin P P, Ding J, Yi JB, Liu B H 2005 *Journal of Alloys and Compounds* **390** 255
- [13] Yokoyama D, Namiki K, Yamada Y J 2006 *Radioanal. Nucl. Chem.* **268** 283
- [14] Pola J, Urbanová M, Pokorná D, Bezdička P, Kupčík J, Křenek T 2014 *RSC Advances* **4** 11543
- [15] Karatodorov S, Mihailov V, Křenek T, Grozeva M 2016 *Journal of Physics: Conference Series* **700** 012001
- [16] Lábár J L 2005 *Ultramicroscopy* **103** 237